Eur. Phys. J. Appl. Phys. **87**, 11301 (2019)

https://doi.org/10.1051/epjap/2019190108

THE EUROPEAN PHYSICAL JOURNAL APPLIED PHYSICS

Regular Article

Surface properties of rare-earth metals and the effects of their substitutional doping on work function of the W(110) surface

Jian Wang[1], Zhijun He[1,*], Jin Nie[2], Xiaoxiao Sun[1], Yu Han[1], Meng Wang[1], Junru Jiang[1], Gaobin Liu[1], Dongchao Qiu[1], and Guoyu Jiang[3]

[1] University of Science and Technology Liaoning, Anshan, Liaoning Province 114051, PR China
[2] State Grid Yingkou Power Supply Company, Yingkou, Liaoning Province 115000, PR China
[3] State Grid Anshan Electric Power Supply Company, AnShan, Liaoning Province 114000, PR China

Received: 2 April 2019 / Received in final form: 18 June 2019 / Accepted: 22 July 2019

Abstract. The surface energy and work function of rare-earth metals (from La to Lu) are studied by the first principles calculations. The obtained values are in good agreement with available experimental data. Motivated by enhanced thermionic emission performance resulting from low work function, we substitutionally doped the rare-earth atoms on W(110) surface to improve the work function. The results show that rare-earth atoms doping can significantly reduce the work function of the W(110) surface, and Eu, Pr and Nd are the three best candidates for work function reduction.

1 Introduction

A rare-earth metal (REM), is a general designation of seventeen chemical elements in the periodic table, including the fifteen lanthanides, as well as scandium and yttrium. The REMs have gained considerable attention and widely used in different fields such as nuclear energy, metallurgy, chemical engineering, electronics, and computer manufacturing, due to their diverse chemical, electrical, metallurgical, magnetic, optical and catalytic properties [1–4].

One of the important applications for REMs is in the field of electron emission. As is well known, tungsten as an important electron emission material has low electron emission efficiency because of the high work function. In order to improve its emission efficiency, doping some metals with low work function is an effective and convenient way. The REMs are promising doped elements due to their low work function and active properties. Electron emission is a surface phenomenon, which is closely related to the surface properties of materials.

Work function and surface energy are important parameters of the surface, and they are very useful to understand a wide range of surface phenomena. The work function is defined as the minimum work required to remove a free electron from the interior of a solid to infinitely far away in vacuum [5], which is related to the surface activity. A surface with low work function is more active. The surface energy is the energy required to split an infinite crystal to two parts, which reflects the stability of the surface. Surface with low surface energy is more stable.

A lot work has been done for the surface properties lot of REMs. Eastman presented photoelectric work functions for a number of metals (including La, Ce, Nd, Sm, Eu and Gd) which were prepared in ultrahigh vacuum, using electron-beam-gun evaporation techniques [6]. Nikolic et al. analyzed the dependence of the work function of rare-earth metals on their electron structure [7]. They presented the average work function of each REM, but did not study the specific values of work functions on different surfaces. Skriver performed an ab initio study of the surface energy and the work function for six close-packed surfaces of 40 elemental metals, but for REMs only La and Lu considered [8]. Vitos used density functional theory to establish a database of surface energies for low index surfaces of 60 metals including 4 rare-earth elements in the periodic table [9].

All these researches are very useful to understand the surfaces properties of the REMs and provide a guide for experiment. However, these studies only focus on 1 or 2 close-packed surfaces and the data are less and incomplete. Therefore, one aim of our paper is to establish a database of the surface properties of REMs.

As mentioned above, an application of the REMS is in the field of electron emission. The experiments show that La and Ce doping on Mo surface can significantly reduce the surface work function and improve the efficiency of electron emission [10]. But for other REMs, the effects of their doping on W surface are not clear, so the second aim of this paper is to clarify the effects to the work function of W(110) surface.

In this paper, we calculated the surface energies and work functions of REMs and discussed the variation of the work function of the most close-packed surfaces. In addition, the work function changes of the W(110) surface

* e-mail: hzj0412@126.com

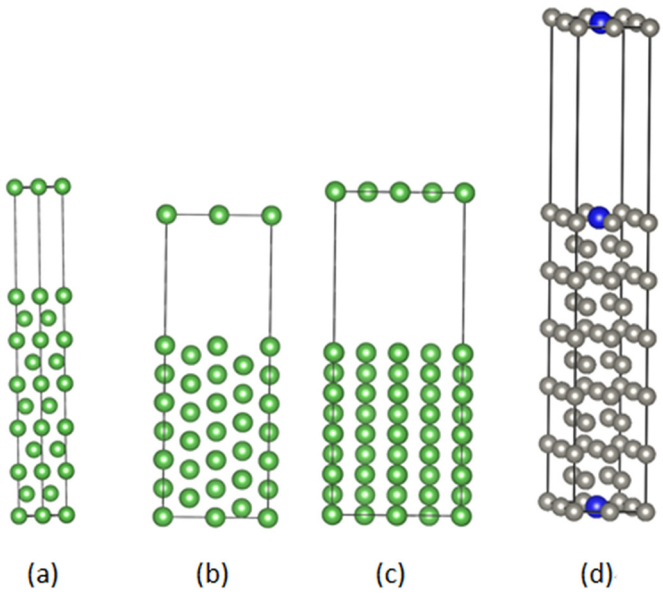

Fig. 1. (a) La(0001) surface (b) La(10–10) surface (c) La(11–20) surface (d)25% lanthanide-doped W(110) surface, the blue sphere stands for lanthanide atom, the grey spheres are W atoms.

after the REMs doping were investigated. Finally, the conclusions were presented.

2 Details and calculation model

The DFT calculations were performed using the Vienna ab initio simulation package (VASP) code [11] with the projector-augmented wave (PAW) approach [12]. The Perdew-Burke-Ernzerhof (PBE) generalized gradient approximation was applied to treat the electronic exchange-correlation effects [13]. The standard slab model was used to simulate the surface, in which periodic boundary conditions are applied to the surface supercell including a slab of atomic layers and a vacuum region as shown in Figure 1, and the thickness of the slab was tested to obtain the converged results. The plane-wave cutoff energy of 400 eV was employed to expand electronic wave functions, the k-point meshes were adjusted according to the size of the slab models to obtain well converged total energies (the specific size of the k-point mesh will be given in Tab. A.1). Spin polarization was not taken into account and the Methfessel–Paxton method was employed to determine electron occupancies with a smearing width of 0.1 eV. In the direction perpendicular to the surface, a 1.5 nm vacuum layer inserted to minimize the surface–surface interaction. In the slab optimizations, the 3–5 layers close to the surface (top and bottom) were allowed to relax and the remaining layers in the center were fixed at their bulk positions. The convergence criterion of the slab structure optimization for ionic relaxations was 10^{-6} eV between successive optimization steps. Using the conjugate gradient method, the top and bottom 3–5 layers were optimized until the atomic forces on each atom were less than 0.02 eV/Å.

2.1 Work function

The work function can be calculated using the following formula [1]:

$$\mathrm{W} = E_{vacuum} - E_F, \tag{1}$$

where E_{vacuum} is the electrostatic potential in the middle of the vacuum region of the slab, E_F stands for the Fermi energy. In our slab model, both of them can be derived from the same calculation.

2.2 Surface energy

Surface energy γ is a measure of the destruction of chemical bonds when creating material surfaces. It can be presented in the following expression [14]:

$$\gamma = \frac{(E_{slab} - NE_{bulk})}{2A},$$

where E_{slab} is the total energy of the slab, N is the number of total atoms, E_{bulk} is the energy per atom in the bulk and A is the area of the slab. "2" in the denominator indicates that two surfaces are involved in the calculations because of three dimensional boundary conditions. It can be seen that the smaller the surface energy, the higher the stability of the surface is.

2.3 Crystal structures and slab models

The lanthanide has three kinds of crystal structure: Ce and Yb are face-centered cubic (FCC) structures, Eu is body-centered cubic (BCC) structures. Correspondingly, a series of $9 \times 9 \times 9$, $9 \times 9 \times 9$ and $11 \times 11 \times 11$ Monkhorst-Pack k-point grids are used for bulk calculations, respectively. The rest of REMs are hexagonal (HCP) structures. In calculations of La, Pr, Nd, Pm and Sm bulk, a mesh size of $8 \times 8 \times 2$ is used for k-point sampling, the others are used $11 \times 11 \times 6$ k-mesh for bulk calculation. Here we build 4 surface slab modes for the FCC and BCC structure metals and 3 surface slabs for HCP structures including (0001), (10–10) and (11–20) surfaces. Take La for example, some of slab models are shown in Figure 1. The calculation details of slab models are relegated to Appendices.

3 Results and discussion

3.1 Surface properties of RMEs

The lattice constants are calculated in the bulk model and the results are listed in Table 1. The c/a ratio and the errors compared with experimental values are also given. We can see that the mean deviation of c/a ratio between our results and experiments is within 3%. It is indicated that our results are in excellent agreement with previous experimental data.

The calculated surface energy and work function results are shown in Table 2 in Jm^{-2} and eV, respectively. For comparison the experimental values available are also listed. It is seen that the work functions present are in good

Table 1. The comparison of the calculated crystal lattices with experimental values.

REMS	Lattice constant			Experimental values [15–17]			$\Delta c/a$ (%)
	a	c	c/a	a	c	c/a	
La	3.780	12.033	3.183	3.772 ± 4	12.144 ± 15	3.219	−1.1
Ce	4.703			$5\ 1606 \pm 5$			
Pr	3.752	11.933	3.180	3.672 ± 2	$11.\ 834 \pm 5$	3.223	−1.3
Nd	3.719	11.836	3.183	3.659 ± 3	11.799 ± 7	3.225	−0.13
Pm	3.684	11.741	3.187	3.65	11.65	3.197	−0.3
Sm	3.659	11.675	3.191	3.626	11.747	3.24	−1.5
Eu	4.464			4.580 ± 2			
Gd	3.632	5.743	1.581	3.634 ± 3	5.781 ± 5	1.591	−0.63
Tb	3.625	5.648	1.558	3.604 ± 4	5.698 ± 3	1.581	−1.5
Dy	3.638	5.597	1.538	3.592 ± 4	5.655 ± 2	1.574	−2.3
Ho	3.622	5.558	1.535	3.578 ± 3	5.626 ± 9	1.572	−2.4
Er	3.601	5.521	1.533	$3.\ 560 \pm 2$	$5.\ 595 \pm 6$	1.572	−2.5
Tm	3.585	5.48	1.529	3.5374 ± 2	$5.\ 558 \pm 4$	1.571	−2.7
Yb	5.452			5.483 ± 3			
Lu	3.505	5.549	1.583	3.505 ± 2	5.553 ± 3	1.584	−0.06

Note: The limits of error for filings are the standard deviations for one determination $\pm 3 = \pm 0.0003$

agreement with the available experimental results, but the calculated surface energies by the present PBE-GGA method are slightly smaller than the experimental values, especially for La. In our previous work [14], we have shown that compared to PBE method, the surface energy calculated by LDA (local density approximation) method is more closed to the experimental values. Therefore, for La, the surface energies of these two kinds of pseudopotentials are given in Table 2, respectively. It can be seen that the surface energy of La metal calculated by LDA method agree better with experiment. For other lanthanide elements, due to the lack of corresponding LDA pseudopotential, we only give the results of PBE calculation.

From Table 2, we also find that the surface energy and the work function of a given metal depend on the crystallographic orientation. The work function of the most close-packed surface (such as (0001) surface of HCP structure) is higher than that of other surfaces. But the surface energy of the most packed surface is almost lower than that of other planes.

As we known, the surface energy reflects the stability of the various surfaces. The lower the surface energy is, the more stable the surface is. So the most close-packed surface is the most stable because of the lowest surface energy, such as (0001) surface for Hcp structure, (110) surface for Bcc structure and (111) surface for Fcc structure. These planes can be selected as representative surfaces to characterize the surface properties of REMs. Therefore, in order to figure out the work function variation with Lanthanide elements, we have made Figure 2, in which the work function of the REMS is represented by that of the most close-packed surface. We Can see that the work function increases in the sequence $W_{Yb} < W_{Eu} < W_{La} < W_{Pr} < W_{Nd} < W_{Er} < W_{Ho} < W_{Dy} < W_{Gd} < W_{Sm} < W_{Pm} < W_{Ce} < W_{Lu} < W_{Tm}$. And Yb, Eu an La have the lower work function, which indicate that they are three most active elements of the REMs. For other REMs, the work functions are similar from Pr to Pm, which show similar active properties. And Ce, Lu and Tm have the higher work functions.

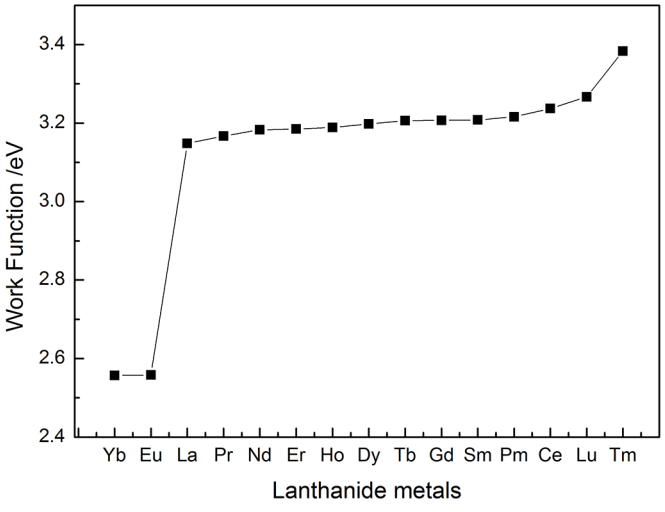

Fig. 2. Work function variation with lanthanide metals.

3.2 Effects of substitutional REMs doping on work function of W(110) surface

From reference [10], We know when La_2O_3 and Sc_2O_3 are doped into Mo matrix, La and Sc atoms are tend to transport to the surface. Enlightened by this phenomenon,

Table 2. Work function W(eV) and surface energy γ (J/m^2) of REMs.

REMs	Surface	W(eV) Present	W(eV) Exp.	γ (J/m^2) Present	γ (J/m^2) Exp.[c]
La	(0001)	3.148	3.5 ± 0.2[a]	0.425^{PBE} 0.926^{LDA}	1.02
	(10–10)	3.064		0.62^{PBE} 0.982^{LDA}	
	(11–20)	2.760		0.624^{PBE} 0.95^{LDA}	
Ce	(100)	3.134	2.9 ± 0.2[a]	1.392	
	(110)	3.025		1.331	
	(111)	3.237		1.333	
	(123)	3.082		1.367	
Pr	(0001)	3.167	2.7[b]	0.749	0.707
	(10–10)	3.034		0.877	
	(11–20)	2.787		0.804	
Nd	(0001)	3.183	3.2[a]	1.286	
	(10–10)	3.037		1.152	
	(11–20)	2.811		1.117	
Pm	(0001)	3.216	3.07[b]	0.795	0.68
	(10–10)	3.05		0.937	
	(11–20)	2.828		0.860	
Sm	(0001)	3.208	2.7 ± 0.3[a]	0.810	
	(10–10)	3.058		0.965	
	(11–20)	2.853		0.887	
Eu	(100)	3.070	2.5 ± 0.3[a]	0.450	
	(110)	2.558		0.454	0.45
	(111)	2.470		0.552	
	(133)	2.520		0.514	
Gd	(0001)	3.207	3.3 ± 0.1[a]	0.742	1.11
	(10–10)	2.824		1.087	
	(11–20)	2.936		0.842	
Tb	(0001)	3.206	3.0[b]	0.769	1.13
	(10–10)	2.802		1.117	
	(11–20)	2.946		0.854	
Dy	(0001)	3.198	3.09[b]	0.704	1.14
	(10–10)	2.783		1.60	
	(11–20)	2.989		0.874	
Ho	(0001)	3.189	3.09[b]	0.786	1.15
	(10–10)	2.780		1.296	
	(11–20)	3.025		0.879	
Er	(0001)	3.185	3.12[b]	0.860	1.17
	(10–10)	2.781		1.186	
	(11–20)	3.029		0.909	
Tm	(0001)	3.383	3.15[b]	0.869	<1.18
	(10–10)	3.416		0.857	
	(11–20)	3.058		0.920	
Yb	(100)	2.523	2.6[b]	0.437	
	(110)	2.649		0.519	
	(111)	2.557		0.455	0.5
	(123)	2.610		0.513	
Lu	(0001)	3.267	3.3[b]	0.887	1.225
	(10–10)	2.771		1.208	
	(11–20)	3.054		0.936	

Notes: [a]Reference [6]. [b]Reference [7]. [c]Reference [18].

Table 3. Work functions of lanthanide doped W(110) surface.

Lanthanide elements	Work function of lanthanide doped surfaces W(eV)	Reduction of work function ΔW(eV)
La	3.108	1.649
Ce	3.656	1.101
Pr	2.471	2.286
Nd	2.559	2.198
Pm	2.650	2.107
Sm	3.179	1.578
Eu	2.346	2.411
Gd	3.613	1.144
Tb	3.703	1.054
Dy	3.818	0.939
Ho	3.879	0.878
Er	3.959	0.798
Tm	4.025	0.732
Yb	2.709	2.048
Lu	4.099	0.658

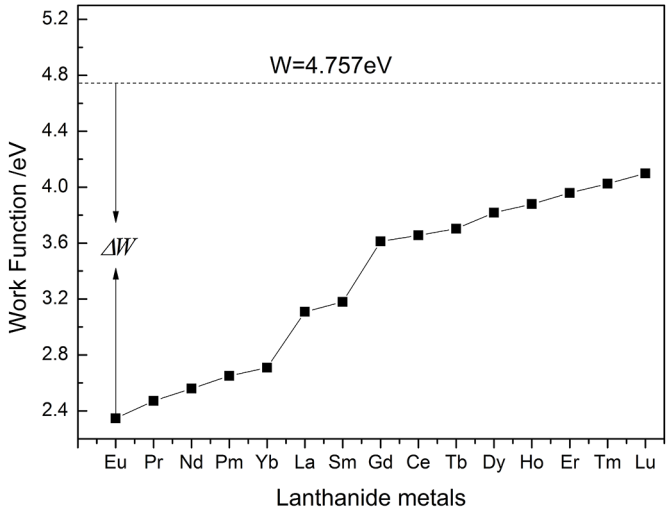

Fig. 3. Work function of lanthanide doped W(110) surface.

in this section, we present a detailed study of the effects of substitutional lanthanide doping on the work function of the W(110) surface. The 2×2 slab mode is selected and it contain 11 layers (4 atoms per layer). The cutoff energy is set to 400 eV and the k points are $6 \times 6 \times 1$. One atom is substituted by the lanthanide atom of the up and down plane to find the optimum doping lanthanide elements, see Figure 1d. For the density of states (DOS), the K points are increased to $10 \times 10 \times 1$, and the tetrahedron method is used to obtain accurate total energy calculations.

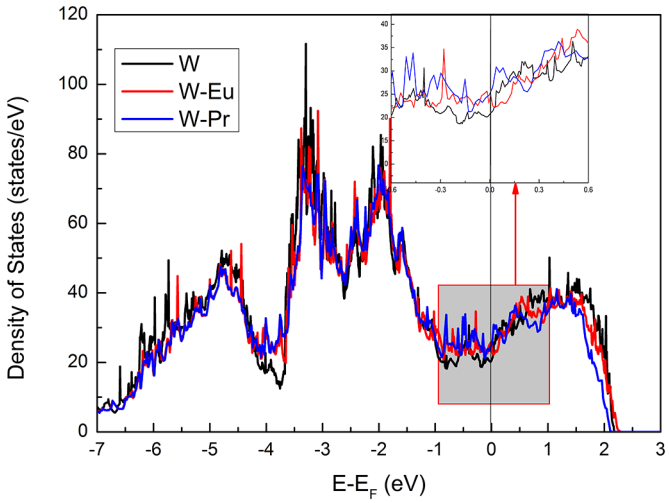

Fig. 4. Total density of states for W(110) clean and Eu, Pr doped surface.

The clean W(110) surface was firstly considered before the lanthanide doping. The work function of the clean surface in our calculation is 4.757 eV, which is in agreement with the experimental results and other theoretical values [14]. After lanthanide doping, the work function changes are listed in Table 3. To further illustrate the decreasing trend, we present Figure 3. It can be found that all lanthanide metals doping can reduce the work function of the W(110) surface. The order of reduction is following: $\Delta W_{Eu} > \Delta W_{Pr} > \Delta W_{Nd} > \Delta W_{Pm} > \Delta W_{Yb} > \Delta W_{La} > \Delta W_{Sm} > \Delta W_{Gd} > \Delta W_{Ce} > \Delta W_{Tb} > \Delta W_{Dy} > \Delta W_{Er} > \Delta W_{Tm}$. The order of reduction can be clearly seen in Figure 3. We can found that Eu, Pr and Nd are three optimum lanthanide elements, which induced the W(110) reduction is 2.411 eV, 2.286 eV and 2.198 eV, respectively.

3.3 Density of states

To further look into the effect of lanthanide doping on the electronic structure of tungsten surface, we calculated the density states (DOS) of clean and Eu, Pr doped W(110) in Figure 4. We can see that the DOS plots of clean and doped surface are similar and their shape and range of DOS values are much closed, which is not too surprising, since the crystal structures are almost identical. From the drawing of partial enlargement in Figure 4, we can find that the three DOS are different at the Fermi level. It is well known that the DOS value at Fermi level is often closely related to the relative stability of crystal, that is, the lower the DOS is, the more stable the corresponding phase is [19–22]. For the surface model, we think the DOS value of Fermi level is correlated with the surface stability. Compared with clean DOS plot, the DOS value of Eu, Pr doped surface is little higher than the clean DOS plot at the Fermi level, which means that the doped surface is more unstable than the clean surface. In other words, the doped surfaces is more active, so they are easier to lose electrons and the work functions are smaller than clean W (110) surface. This may be one of the reasons for the decrease of the work function.

4 Conclusion

We calculate the work functions and surface energies of various crystal planes of REMs using the first-principles calculations based on the DFT. The calculated results are in good agreement with the available experimental values. In terms of surface energy, the (0001) surface is always the smallest one for HCP structure, which indicates that this surface is the most stable, so is (110) surface of BCC structure and (111) surface of FCC structure. For the work function, the increasing order of the REMs is discussed, which follows $W_{Yb} < W_{Eu} < W_{La} < W_{Pr} < W_{Nd} < W_{Er} < W_{Ho} < W_{Dy} < W_{Gd} < W_{Sm} < W_{Pm} < W_{Ce} < W_{Lu} < W_{Tm}$.

Motivated by enhanced thermionic emission performance resulting from low work function, we substituted 25% of surface sites of W(110) with the rare earth elements and studied the work function changes induced by lanthanide doping. The calculation indicates that all lanthanide metals can reduce the work function, and Eu, Pr and Nd are three optimum candidate elements. Take W-Eu, W-Pr surface for example, we reveal the reason for the decrease of work function by analyzing the DOS value near Fermi level.

This work was supported in part by the National Natural Science Foundation of China under Grant Nos. 51874171, the Liaoning Natural Science Foundation No. 20180550698, the University of Science and Technology Liaoning Foundation Project No. 2018RC01 and 2017QN02. This work is also supported by 2019 joint fund of SKLMEA and USTL, the project number is SKLMEA-USTLN-201904.

Author contribution statement

Jian Wang and Zhijun He made substantial contributions to drafting the article, designing the calculations. Jin Nie and Xiaoxiao Sun performed all the calculations. Yu Han, Meng Wang and Junru Jiang programmed the data treatment software. Gaobin Liu, Dongchao Qiu and Guoyu Jiang supervised the project and revised the manuscript. All authors discussed the results and approved the final manuscript.

References

1. N. Haque, A. Hughes, S. Lim, C. Vernon, Resources **3**, 614 (2014)
2. X. Du, T.E. Graedel, Sci. Total Environ. **461–462**, 781 (2013)
3. S. Massari, M. Ruberti, Resour. Policy **38**, 36 (2013)
4. A.R. Chakhmouradian, F. Wall, Elements **8**, 333 (2012)
5. A. Kahn, Mater. Horiz. **3**, 7 (2016)
6. D. Eastman, Phys. Rev. B **2**, 1 (1970)
7. M. Nikolić, S. Radić, V. Minić, M. Ristić, Microelectr. J. **27**, 93 (1996)
8. H.L. Skriver, N. Rosengaard, Phys. Rev. B **46**, 7157 (1992)
9. L. Vitos, A.V. Ruban, H.L. Skriver, J. Kollár, Surf. Sci. **411**, 186 (1998)
10. J. Yang, Z. Nie, Y. Wang, Appl. Surf. Sci. **215**, 87 (2003)
11. G. Kresse, J. Furthmüller, Phys. Rev. B **54**, 11169 (1996)
12. P.E. Blöchl, Phys. Rev. B **50**, 17953 (1994)
13. J.P. Perdew, K. Burke, M. Ernzerhof, Phys. Rev. Lett. **77**, 3865 (1996)
14. J. Wang, S.-Q. Wang, Surf. Sci. **630**, 216 (2014)
15. B. Beaudry, P. Palmer, J. Less Common Metals **34**, 225 (1974)
16. F.H. Spedding, A. Daane, K. Herrmann, Acta Crystallogr. **9**, 559 (1956)
17. K. Gschneidner, J. Phase Equilib. **11**, 216 (1990)
18. F. De Boer, R. Boom, W. Mattens, A. Miedema, A. Niessen, *Cohesion in Metals* (North-Holland, Amsterdam, 1988)
19. J. Nylén, F.J. Garcìa Garcìa, B.D. Mosel, R. Pöttgen, U. Häussermann, Solid State Sci. **6**, 147 (2004)
20. D.W. Zhou, P. Peng, J.S. Liu, J. Alloy Compd. **428**, 316 (2007)
21. C. Fu, X. Wang, Y. Ye, K. Ho, Intermetallics **7**, 179 (1999)
22. A. Vakhney, A. Yaresko, V. Antonov, V. Nemoshkalenko, Int. J. Hydrogen Energ. **26**, 453 (2001)

Cite this article as: Jian Wang, Zhijun He, Jin Nie, Xiaoxiao Sun, Yu Han, Meng Wang, Junru Jiang, Gaobin Liu, Dongchao Qiu, Guoyu Jiang, Surface properties of rare-earth metals and the effects of their substitutional doping on work function of the W(110) surface, Eur. Phys. J. Appl. Phys. **87**, 11301 (2019)

Appendix A

Table A.1. Computational details of various slab models.

REMs	Surface orientation	Atom layers	Atom numbers	Slab thickness (Å)	Size of the unit-cell (a,b,c) (Å), (α, β, γ) (°)	K mesh	Valence for each atomic species
La	(0001)	15	15	42.105	(3.779,3.779,57.105) (90,90,60)	14 × 14 × 1	11
	(10–10)	26	26	19.640	(3.779,12.03, 34.64) (90,90,90)	9 × 3 × 1	
	(11–20)	13	52	22.679	(12.03,6.547,37.679) (90,90,90)	3 × 6 × 1	
Ce	(100)	11	11	23.510	(3.325,3.325,38.515) (90,90,90)	10 × 10 × 1	12
	(110)	11	11	16.628	(4.703,3.326,31.628) (90,90,90)	6 × 10 × 1	
	(111)	13	13	32.583	(3.326,3.326,47.583) (90,90,120)	14 × 14 × 1	
	(123)	29	29	17.597	(5.760,7.436,32.597) (90,90,75)	6 × 5 × 1	
Pr	(0001)	15	15	41.765	(3.752,3.752,56.766) (90,90,120)	14 × 14 × 1	11
	(10–10)	19	26	19.496	(3.752,11.933,34.496) (90,90,90)	10 × 3 × 1	
	(11–20)	13	52	22.512	(11.933,6.499,37.512) (90,90,90)	3 × 6 × 1	
Nd	(0001)	15	15	41.426	(3.719,3.719,56.426) (90,90,120)	14 × 14 × 1	11
	(10–10)	19	26	19.324	(3.719,11.836,34.325) (90,90,90)	10 × 3 × 1	
	(11–20)	13	52	22.314	(11.836,6.442,37.314) (90,90,90)	3 × 6 × 1	
Pm	(0001)	15	15	41.091	(3.684,3.684,56.091) (90,90,120)	14 × 14 × 1	11
	(10–10)	19	26	19.143	(3.684,11.740,34.143) (90,90,90)	10 × 3 × 1	
	(11–20)	13	52	22.104	(11.740,6.381,37.104) (90,90,90)	3 × 6 × 1	
Sm	(0001)	15	15	40.862	(3.659,3.659,55.863) (90,90,120)	14 × 14 × 1	11
	(10–10)	19	26	19.013	(3.659,11.675,34.013) (90,90,90)	10 × 3 × 1	
	(11–20)	13	52	21.954	(11.675,6.338,36.954) (90,90,90)	3 × 6 × 1	
Eu	(100)	13	13	26.760	(4.460,4.460,41.759) (90,90,90)	10 × 10 × 1	8
	(110)	11	11	31.537	(3.862,3.862,46.537) (90,90,70.5)	14 × 14 × 1	
	(111)	13	13	15.464	(6.313,6.313,30.464) (90, 90,120)	6 × 6 × 1	
	(133)	39	39	19.441	(14.404,6.307,34.441) (90,90,102.9)	4 × 8 × 1	
Gd	(0001)	14	14	36.777	(3.673,3.673,51.777) (90,90,120)	14 × 14 × 1	9
	(10–10)	18	18	27.584	(3.673,5.658,42.568) (90,90,90)	10 × 7 × 1	
	(11–20)	13	26	22.038	(5.658,6.362,37.038) (90,90,90)	7 × 6 × 1	

Table A.1. (continued).

REMs	Surface orientation	Atom layers	Atom numbers	Slab thickness (Å)	Size of the unit-cell (a,b,c) (Å), (α, β, γ) (°)	K mesh	Valence for each atomic species
Tb	(0001)	14	14	36.548	(3.651,3.651,51.550) (90,90,120)	14 × 14 × 1	9
	(10–10)	18	18	27.392	(3.651,5.623,42.403) (90,90,90)	11 × 8 × 1	
	(11–20)	13	26	21.906	(5.623,6.324,36.906) (90,90,90)	6 × 5 × 1	
Dy	(0001)	14	14	36.378	(3.638,3.638,51.381) (90,90,120)	14 × 14 × 1	9
	(10–10)	18	18	27.305	(3.638,5.597,42.307) (90,90,90)	10 × 6 × 1	
	(11–20)	13	26	21.828	(5.597,6.301,36.828) (90,90,90)	6 × 5 × 1	
Ho	(0001)	14	14	36.147	(3.622,3.622,51.127) (90,90,120)	14 × 14 × 1	9
	(10–10)	18	18	27.167	(3.622,5.558,42.185) (90,90,90)	10 × 6 × 1	
	(11–20)	13	26	21.732	(5.558,6.234,36.732) (90,90,90)	6 × 5 × 1	
Er	(0001)	11	11	27.565	(3.601,3.601,42.605) (90,90,120)	14 × 14 × 1	9
	(10–10)	18	18	27.019	(3.601,5.520,42.020) (90,90,90)	10 × 6 × 1	
	(11–20)	13	26	21.560	(5.520,6.235,36.600) (90,90,90)	6 × 5 × 1	
Tm	(0001)	13	13	32.894	(3.585,3.585,47.880) (90,90,120)	14 × 14 × 1	9
	(10–10)	18	18	26.909	(3.585,5.480,41.909) (90,90,90)	10 × 6 × 1	
	(11–20)	13	26	21.510	(5.480,6.209,36.510) (90,90,90)	6 × 5 × 1	
Yb	(100)	11	11	27.265	(3.856,3.856,42.265) (90,90,90)	13 × 13 × 1	8
	(110)	13	13	23.135	(5.453,3.856,38.135) (90,90,90)	7 × 9 × 1	
	(111)	10	10	28.335	(3.856,3.856,43.335) (90,90,120)	13 × 13 × 1	
	(123)	29	29	20.403	(6.679,8.622,35.403) (90,90,75)	6 × 4 × 1	
Lu	(0001)	14	14	36.052	(3.505,3.505,51.066) (90,90,120)	14 × 14 × 1	9
	(10–10)	18	18	26.904	(3.585,5.480,41.907) (90,90,90)	10 × 7 × 1	
	(11–20)	13	26	21.510	(5.480,6.209,36.510) (90,90,90)	6 × 5 × 1	
W	(110)	11	44	22.224	(5.444,5.444,37.224) (90,90,70.5)	6 × 6 × 1	6